

CHAPTER 2

RADIATIVE FLOW PAST A PARABOLIC STARTED ISOTHERMAL VERTICAL PLATE WITH UNIFORM MASS FLUX

2.1 INTRODUCTION

The study of radiative heat and mass transfer in convective flows is important from many industrial and technological points of view. Mass transfer is one of the most commonly encountered phenomena in chemical industry as well as in physical and biological sciences. A few representative fields of interest in which combined heat and mass transfer plays an important role are designing chemical processing equipment, formation and dispersion of fog, distribution of temperature and moisture over agricultural fields and groves of fruit trees, crop damage due to freezing, and environmental pollution.

The radiative heat and mass transfer flow of an electrically conducting fluid has wide applications in geophysics, geothermal, engineering and solar physics. It plays an important role in manufacturing industries for the design of fins, steel rolling, nuclear power plants, gas turbines and various propulsion device for space vehicles, aircraft, missiles, energy conversion methods that involve fossil fuel combustion, solar radiation and furnace design, satellites, materials processing, energy utilization, temperature measurements, remote sensing for astronomy and space exploration, food processing and cryogenic engineering, as well as numerous agricultural, health and military applications.

Soundalgekar (1982) studied the mass transfer effects on flow past a uniformly accelerated vertical plate. Mass transfer effects on flow past an accelerated vertical

plate with uniform heat flux was analyzed by Singh & Singh (1983). The dimensionless governing equations were solved using the Laplacetransform technique. We observed that a close study of the table indicates that as the Schmidt number increases the skin friction decreases. Thus the skin-friction is greater in the case of hydrogen than in the case of water vapor and oxygen.

Cess (1966) investigated thermal radiation effects on heated vertical plate using singular perturbation technique. Natural convection on flow past an linearly accelerated vertical plate in the presence of viscous dissipative heat using perturbation method examined by Gupta et al (1979). Kafousias & Raptis (1981) extended this problem to include mass transfer effects subjected to variable suction or injection. The dimensionless governing equations were solved by numerical methods. It was observed that the suction or injection on the flow field has been extensively discussed when the plate is being cooled or heated by the free convection currents.

The radiation effect on convective flow and heat transfer problems has become more important industrially. Free convection flow involving coupled heat and mass transfer occurs frequently in nature and in industrial processes. Free convection effects on flow past an exponentially accelerated vertical plate was studied by Singh & Naveen Kumar (1984). The skin friction for accelerated vertical plate has been studied analytically by Hossain & Shayo (1986). Mass transfer effects on exponentially accelerated infinite vertical plate with constant heat flux and uniform mass diffusion was studied by Basant Kumar Jha et al (1991).

Hossain & Takhar (1996) have analyzed radiation effects on mixed convection along an isothermal vertical plate. Agrawal et al (1998) studied free convection due to thermal and mass diffusion in laminar flow of an accelerated infinite vertical

plate in the presence of magnetic field. Agrawal et al (1999) further extended the problem of unsteady free convective flow and mass diffusion of an electrically conducting elasto-viscous fluid past a parabolic starting motion of the infinite vertical plate with transverse magnetic plate. The governing equations are tackled using Laplace transform technique.

Raptis & Perdikis (1999) have studied the effects of thermal radiation and free convection flow past a moving vertical plate. The governing equations were solved analytically. Muthucumaraswamy & Saravanan (2013) have discussed unsteady flow past an oscillating semi-infinite vertical plate of uniform mass flux with thermal radiation using implicit finite difference scheme. If the temperature of the surrounding fluid is rather high, radiation effects play an important role and this situation does exist in space technology. In such cases, one has to take into account the combined effect of thermal radiation and mass flux.

It is proposed to study the effects of on flow past an infinite isothermal vertical plate subjected to parabolic motion with uniform mass flux, in the presence of thermal radiation. The dimensionless governing equations are solved using the Laplace-transform technique. The solutions are in terms of exponential and complementary error function.

2.2 MATHEMATICAL ANALYSIS

Thermal radiation effects on unsteady flow of a viscous incompressible fluid past an infinite isothermal vertical plate with uniform mass flux has been considered. The x -axis is taken along the plate in the vertically upward direction and the y -axis is taken normal to the plate. At time $t' \leq 0$, the plate and fluid are at the same temperature T_∞ and concentration C'_∞ . At time $t' > 0$, the plate is

started with a velocity $u = u_0 t'^2$ in its own plane against gravitational field and the temperature from the plate is raised to T_w and the concentration level near the plate are also raised at an uniform rate. The plate is infinite in length all the terms in the governing equations will be independent of x and are functions of y and t' only. The fluid considered here is a gray, absorbing-emitting radiation but a non-scattering medium. Under the usual Boussinesq's approximation the unsteady flow is governed by the following equations:

$$\frac{\partial u}{\partial t'} = \mathbf{g} \beta (T - T_\infty) + \mathbf{g} \beta^* (C' - C'_\infty) + \nu \frac{\partial^2 u}{\partial y^2} \quad (2.1)$$

$$\rho C_p \frac{\partial T}{\partial t'} = k \frac{\partial^2 T}{\partial y^2} - \frac{\partial q_r}{\partial y} \quad (2.2)$$

$$\frac{\partial C'}{\partial t'} = D \frac{\partial^2 C'}{\partial y^2} \quad (2.3)$$

With the following initial and boundary conditions:

$$u = 0, \quad T = T_\infty, \quad C' = C'_\infty \quad \text{for all } y, \quad t' \leq 0$$

$$t' > 0 : \quad u = u_0 t'^2, \quad T = T_w, \quad \frac{\partial C'}{\partial y} = -\frac{j''}{D} \quad \text{at } y = 0 \quad (2.4)$$

$$u \rightarrow 0, \quad T \rightarrow T_\infty, \quad C' \rightarrow C'_\infty \quad \text{as } y \rightarrow \infty$$

The local radiant for the case of an optically thin gray gas is expressed by

$$\frac{\partial q_r}{\partial y} = -4a^* \sigma (T_\infty^4 - T^4) \quad (2.5)$$

It is assumed that the temperature differences within the flow are sufficiently small such that T^4 may be expressed as a linear function of the temperature. This is accomplished by expanding T^4 in a Taylor series about T_∞ and neglecting higher-order terms, thus

$$T^4 \cong 4T_\infty^3 T - 3T_\infty^4 \quad (2.6)$$

By using Equations (2.5) and (2.6) in Equation (2.2), reduces to

$$\rho C_p \frac{\partial T}{\partial t'} = k \frac{\partial^2 T}{\partial y^2} + 16a^* \sigma T_\infty^3 (T_\infty - T) \quad (2.7)$$

The dimensional quantities are defined as

$$U = u \left(\frac{u_0}{\nu^2} \right)^{\frac{1}{3}}, \quad t = \left(\frac{u_0^2}{\nu} \right)^{\frac{1}{3}} t',$$

$$Y = y \left(\frac{u_0}{\nu^2} \right)^{\frac{1}{3}}, \quad \theta = \frac{T - T_\infty}{T_w - T_\infty},$$

$$C = \frac{C' - C'_\infty}{\left(\frac{j'' \nu^{\frac{2}{3}}}{D u_0^{\frac{1}{3}}} \right)}, \quad Gr = \frac{\mathbf{g} \beta (T_w - T_\infty)}{(\nu u_0)^{\frac{1}{3}}},$$

$$Gc = \frac{\mathbf{g} \beta^* \left(\frac{j'' \nu^{\frac{2}{3}}}{D u_0^{\frac{1}{3}}} \right)}{(\nu u_0)^{\frac{1}{3}}}, \quad R = \frac{16 a^* \sigma T_\infty^3}{k} \left(\frac{\nu^2}{u_0} \right)^{\frac{2}{3}},$$

$$Pr = \frac{\mu C_p}{k} \quad \text{and} \quad Sc = \frac{\nu}{D}.$$

Using in the Equations (2.1), (2.3) and (2.7), reduce to the following dimensionless form:

$$\frac{\partial U}{\partial t} = Gr \theta + Gc C + \frac{\partial^2 U}{\partial Y^2} \quad (2.8)$$

$$\frac{\partial \theta}{\partial t} = \frac{1}{Pr} \frac{\partial^2 \theta}{\partial Y^2} - \frac{R}{Pr} \theta \quad (2.9)$$

$$\frac{\partial C}{\partial t} = \frac{1}{Sc} \frac{\partial^2 C}{\partial Y^2} \quad (2.10)$$

The negative sign in last term of Equation (2.9) indicates that the radiation takes from higher region to lower region.

The initial and boundary conditions in non-dimensional quantities are

$$U = 0, \theta = 0, C = 0 \text{ for all } Y, t \leq 0$$

$$t > 0 : U = t^2, \theta = 1, \frac{\partial C}{\partial Y} = -1 \text{ at } Y = 0 \quad (2.11)$$

$$U \rightarrow 0, \theta \rightarrow 0, C \rightarrow 0 \text{ as } Y \rightarrow \infty$$

2.3 METHOD OF SOLUTION

The Laplace transform method solves differential equations and corresponding initial and boundary value problem. The Laplace transform has the advantage that it solves problems directly, initial value problems without determining first a general solution and non-homogeneous differential equations without solving first

the corresponding homogeneous equations. In order to obtain the exact solution of the present problem, we will use the Laplace transform technique.

On taking Laplace transform of Equations (2.8) to (2.10) and the corresponding initial and boundary conditions Equation (2.11), we get

$$\frac{d^2\bar{U}}{dY^2} - S \bar{U} = -Gr \bar{\theta} - Gc \bar{C} \quad (2.12)$$

$$\frac{d^2\bar{\theta}}{dY^2} - (PrS + R) \bar{\theta} = 0 \quad (2.13)$$

$$\frac{d^2\bar{C}}{dY^2} - Sc S \bar{C} = 0 \quad (2.14)$$

The corresponding transformed boundary conditions are

$$t > 0 : \bar{U} = \frac{2}{S^3}, \quad \bar{\theta} = \frac{1}{S}, \quad \frac{d\bar{C}}{dY} = -\frac{1}{S} \quad \text{at } Y = 0 \quad (2.15)$$

$$\bar{U} \rightarrow 0, \quad \bar{\theta} \rightarrow 0, \quad \bar{C} \rightarrow 0 \quad \text{as } Y \rightarrow \infty$$

where S is the Laplace-transform parameter.

Here $\bar{U}(Y, S)$, $\bar{\theta}(Y, S)$ and $\bar{C}(Y, S)$ denote the Laplace transforms of $U(Y, t)$, $\theta(Y, t)$ and $C(Y, t)$ respectively.

Solving Equations (2.12) to (2.14) subject to the boundary condition Equation (2.15), we get

$$\begin{aligned}
\bar{U} = & \frac{2}{S^3} \exp(-\sqrt{S} Y) + \frac{Gr}{b(1-Pr)} \frac{\exp(-\sqrt{S} Y)}{S} - \frac{Gr}{b(1-Pr)} \frac{\exp(-\sqrt{S} Y)}{S-b} \\
& - \frac{Gc}{1-Sc} \frac{1}{\sqrt{Sc}} \frac{\exp(-\sqrt{S} Y)}{S^{\frac{5}{2}}} - \frac{Gr}{b(1-Pr)} \frac{\exp(-\sqrt{Pr} \sqrt{S+a} Y)}{S} \\
& + \frac{Gr}{b(1-Pr)} \frac{\exp(-\sqrt{Pr} \sqrt{S+a} Y)}{S-b} + \frac{Gc}{1-Sc} \frac{1}{\sqrt{Sc}} \frac{\exp(-\sqrt{Sc} \sqrt{S} Y)}{S^{\frac{5}{2}}},
\end{aligned} \tag{2.16}$$

$$\bar{\theta} = \frac{\exp(-\sqrt{Pr} \sqrt{S+a} Y)}{S} \tag{2.17}$$

and

$$\bar{C} = \frac{\exp(-\sqrt{Sc} \sqrt{S} Y)}{S^{\frac{3}{2}} \sqrt{Sc}} \tag{2.18}$$

On taking inverse Laplace transform of Equations (2.16) to (2.18) and using the standard Laplace transform formula from Table (2.1), we get

$$\begin{aligned}
U = & \frac{t^2}{3} \left[(3 + 12\eta^2 + 4\eta^4) \operatorname{erfc}(\eta) - \frac{\eta}{\sqrt{\pi}} (10 + 4\eta^2) \exp(-\eta^2) \right] + 2d \operatorname{erfc}(\eta) \\
& - d \exp(bt) \left[\exp(2\eta\sqrt{bt}) \operatorname{erfc}(\eta + \sqrt{bt}) + \exp(-2\eta\sqrt{bt}) \operatorname{erfc}(\eta - \sqrt{bt}) \right] \\
& - et\sqrt{t} \left[\frac{4}{\sqrt{\pi}} (1 + \eta^2) \exp(-\eta^2) - \frac{4}{\sqrt{\pi}} (1 + \eta^2 Sc) \exp(-\eta^2 Sc) \right. \\
& \quad \left. - \eta(6 + 4\eta^2) \operatorname{erfc}(\eta) + \eta\sqrt{Sc}(6 + 4\eta^2 Sc) \operatorname{erfc}(\eta\sqrt{Sc}) \right] \\
& - d \left[\exp\left(2\eta\sqrt{Pr at}\right) \operatorname{erfc}\left(\eta\sqrt{Pr} + \sqrt{at}\right) \right. \\
& \quad \left. + \exp\left(-2\eta\sqrt{Pr at}\right) \operatorname{erfc}\left(\eta\sqrt{Pr} - \sqrt{at}\right) \right] \\
& + d \exp(bt) \left[\exp\left(2\eta\sqrt{Pr(a+b)t}\right) \operatorname{erfc}\left(\eta\sqrt{Pr} + \sqrt{(a+b)t}\right) + \right. \\
& \quad \left. \exp\left(-2\eta\sqrt{Pr(a+b)t}\right) \operatorname{erfc}\left(\eta\sqrt{Pr} - \sqrt{(a+b)t}\right) \right],
\end{aligned} \tag{2.19}$$

$$\begin{aligned}
\theta = & \frac{1}{2} \left[\exp\left(2\eta\sqrt{Pr at}\right) \operatorname{erfc}\left(\eta\sqrt{Pr} + \sqrt{at}\right) \right. \\
& \left. + \exp\left(-2\eta\sqrt{Pr at}\right) \operatorname{erfc}\left(\eta\sqrt{Pr} - \sqrt{at}\right) \right]
\end{aligned} \tag{2.20}$$

and

$$C = 2\sqrt{t} \left[\frac{\exp(-\eta^2 Sc)}{\sqrt{\pi} \sqrt{Sc}} - \eta \operatorname{erfc}(\eta \sqrt{Sc}) \right] \quad (2.21)$$

where

$$a = \frac{R}{Pr}, \quad b = \frac{R}{1 - Pr}, \quad d = \frac{Gr}{2b(1 - Pr)}, \quad e = \frac{Gc}{3(1 - Sc)\sqrt{Sc}}$$

and

$$\eta = \frac{Y}{2\sqrt{t}}.$$

Table 2.1 Inverse Laplace transform formula.

	$F(S) = L\{f(t)\}$	$f(t)$
1	$\frac{1}{S} \exp(-Y \sqrt{S})$	$\operatorname{erfc}\left(\frac{Y}{2\sqrt{t}}\right)$
2	$\frac{1}{S^2} \exp(-Y \sqrt{S})$	$\left(\frac{Y^2}{2} + t\right) \operatorname{erfc}\left(\frac{Y}{2\sqrt{t}}\right) - Y \sqrt{\frac{t}{\pi}} \exp\left(\frac{-Y^2}{4t}\right)$
3	$\frac{1}{S-b} \exp(-Y \sqrt{S})$	$\frac{\exp(bt)}{2} \left[\exp(Y\sqrt{b}) \operatorname{erfc}\left(\frac{Y}{2\sqrt{t}} + \sqrt{bt}\right) + \exp(-Y\sqrt{b}) \operatorname{erfc}\left(\frac{Y}{2\sqrt{t}} - \sqrt{bt}\right) \right]$
4	$\frac{1}{S^{\frac{3}{2}}} \exp(-Y \sqrt{S})$	$2 \sqrt{\frac{t}{\pi}} \exp\left(\frac{-Y^2}{4t}\right) - Y \operatorname{erfc}\left(\frac{Y}{2\sqrt{t}}\right)$
5	$\frac{1}{S} \exp(-Y \sqrt{S+b})$	$\frac{\exp(-Y\sqrt{b})}{2} \operatorname{erfc}\left(\frac{Y}{2\sqrt{t}} - \sqrt{bt}\right) + \frac{\exp(Y\sqrt{b})}{2} \operatorname{erfc}\left(\frac{Y}{2\sqrt{t}} + \sqrt{bt}\right)$
6	$\frac{1}{S-b} \exp(-Y \sqrt{S+a})$	$\frac{1}{2} \exp(bt) \left[\exp(Y\sqrt{a+b}) \operatorname{erfc}\left(\frac{Y}{2\sqrt{t}} + \sqrt{(a+b)t}\right) + \exp(-Y\sqrt{a+b}) \operatorname{erfc}\left(\frac{Y}{2\sqrt{t}} - \sqrt{(a+b)t}\right) \right]$

2.4 NUMERICAL RESULTS AND DISCUSSION

In order to determine the effect of different physical parameters such as Gr , Gc , R , Sc and t on the problem, the numerical values of the temperature field, concentration and velocity profile were computed and are shown in the figures. The value of the Prandtl number Pr is taken as 0.71 which represent air.

The numerical values of the Schmidt number Sc are chosen such that they represent a reality in case of air. The effect of Schmidt number play an important role in the concentration. The numerical values of the Schmidt number are chosen to represent the presence of species by hydrogen H_2 (0.16), Heleum He (0.3), Water vapor H_2O (0.6) and Ethyl Benzene $C_6H_5CH_2CH_3$ (2.01).

2.4.1 Effect on temperature distribution

The temperature profiles are plotted in Figure 2.1 for different values of thermal radiation parameter R with $t = 0.2$. The effect of thermal radiation parameter is important in the temperature profiles. It is observed that an increase in the radiation parameter marginally decreases the temperature. This shows that the heat loss is more due to higher thermal radiation.

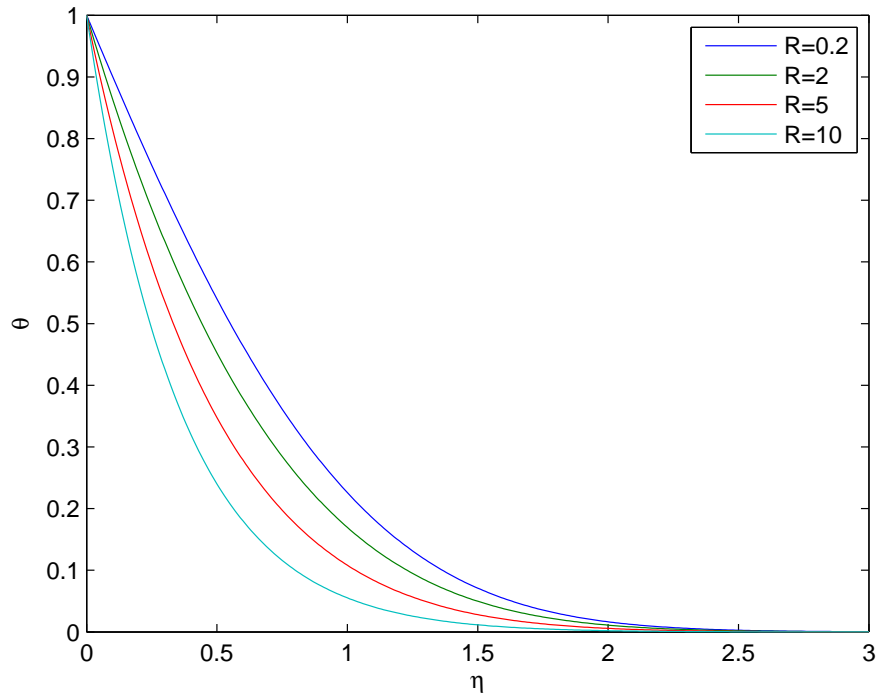


Figure 2.1 Temperature profile for different values of radiation parameter R

2.4.2 Effect on concentration field

The effect of Schmidt number is important in concentration field. The profiles have the common feature that the concentration decreases in a monotone fashion from the surface to a zero value far away in the free stream. Figure 2.2 represents the effect of concentration profiles for different Schmidt number Sc with time $t = 0.2$. It is noted that all other participating parameters are held constant and the concentration of the fluid is enhanced with the decreasing value of Schmidt number. This causes the concentration buoyancy effects to decrease yielding a reduction in the fluid velocity. A reduction in the concentration distribution is accompanied by simultaneous reduction in the concentration boundary layer.

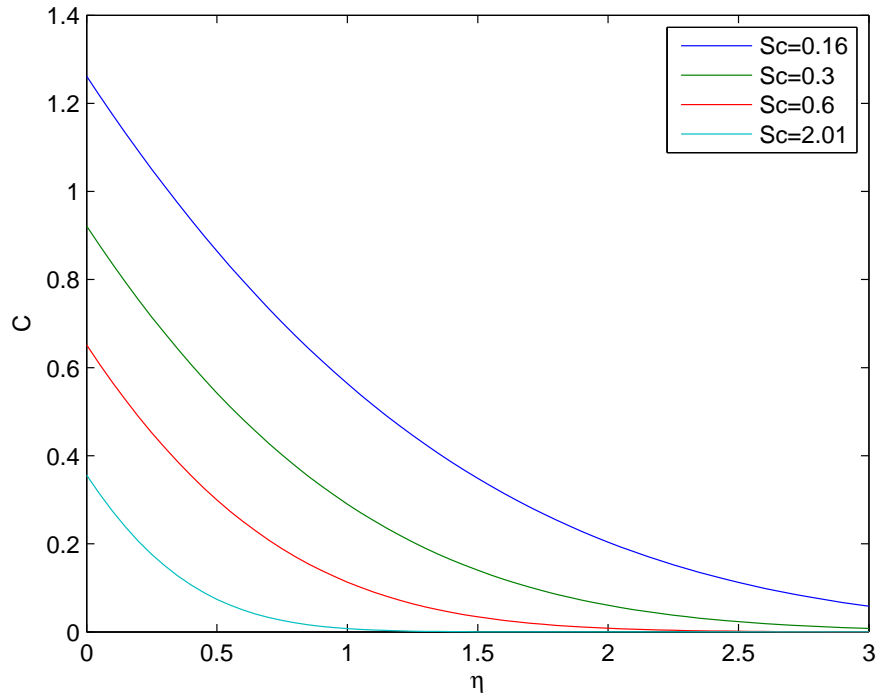


Figure 2.2 Concentration profile for different values of Sc

2.4.3 Effect on velocity profiles

The effect of velocity for different values of the radiation parameter $R = 0.2, 2, 5, 10$ with $Gr = 5 = Gc$, $Sc = 0.6$ and $t = 0.2$ are shown in Figure 2.3. It is clear that the velocity increases considerably as radiation parameter decreases. The trend shows that the velocity increases rapidly and attains maximum value around $\eta = 0.5$, then decreases gradually at $\eta = 2.5$ from which steadily upto $\eta = 3$. Also, it is seen that the velocity decreases in the presence of high thermal radiation. This shows that the buoyancy effect on the temperature distribution is very significant in the air.

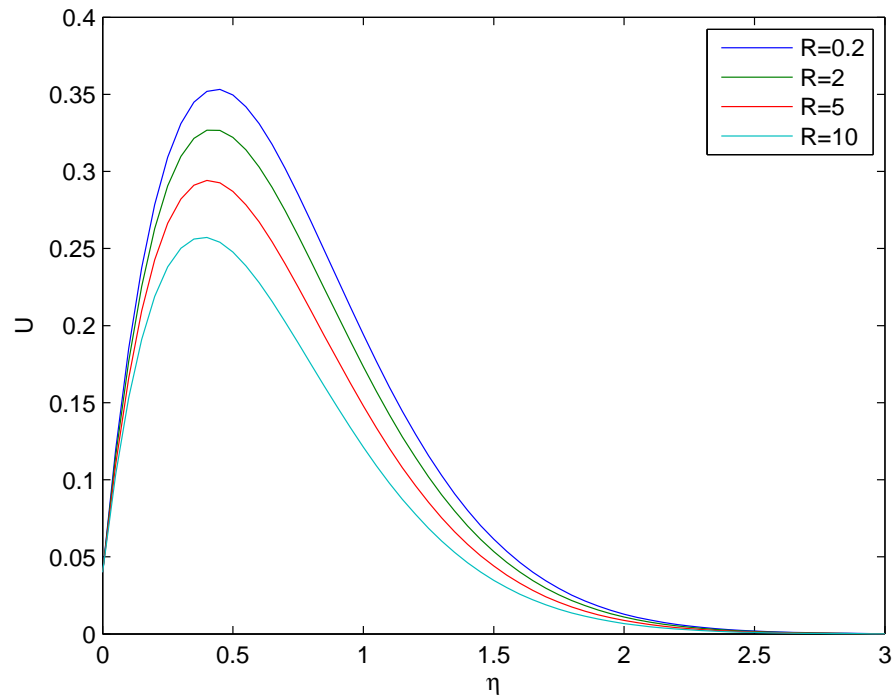


Figure 2.3 Velocity profile for different values of R

Figure 2.4 describes the behavior of the transient velocity with changes in the values of Schmidt number Sc for $t = 0.2$. The velocity decreases considerably due to an increase in Sc . It is found that velocity increases rapidly and attains maximum value at $\eta = 0.5$, and then decreases gradually for increasing values of η . The velocity boundary layer seems to grow in the direction of motion of the plate.

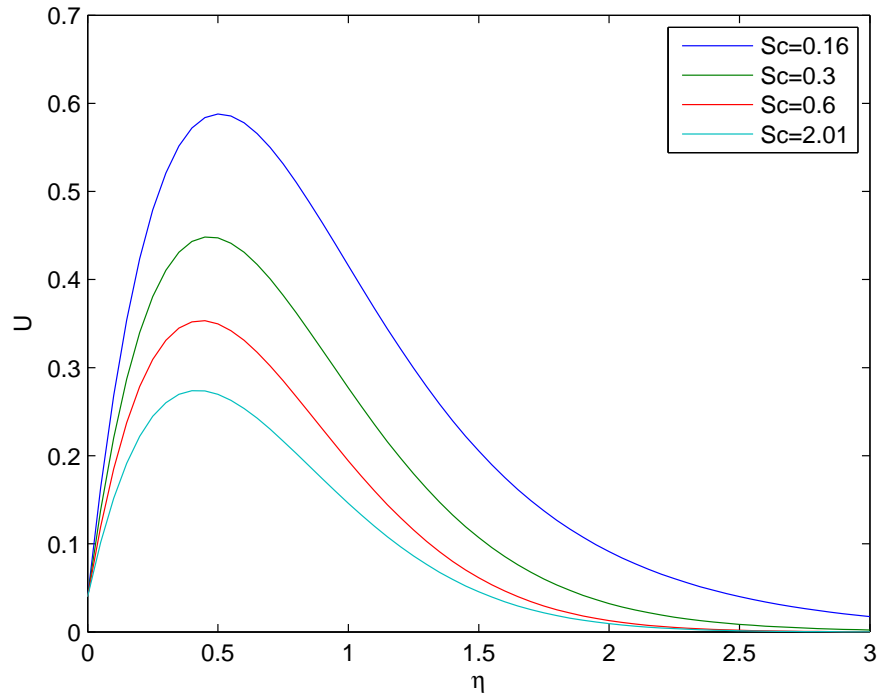


Figure 2.4 Velocity profile for different values of Sc

The effects of different thermal Grashof number $Gr = 2, 5$ and mass Grashof number $Gc = 5, 10$ on the velocity profile with $t = 0.2$ is sketched in Figure 2.5. The thermal Grashof number signifies the relative effect of the enhancement in buoyancy force to the viscous hydrodynamic force and the mass Grashof number defines the ratio of the species buoyancy force to the viscous hydrodynamic force. It is observed that the velocity increases significantly with increasing values of the thermal Grashof number and mass Grashof number. It is seen that the peak values of the velocity increases rapidly near the plate as thermal Grashof number and mass Grashof number increases and then decays to the free stream velocity.

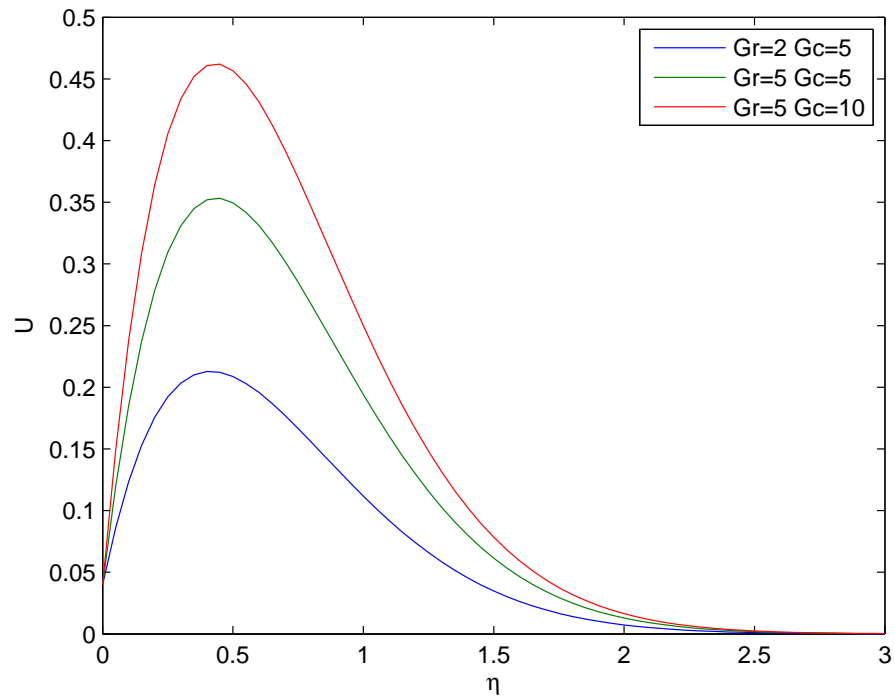


Figure 2.5 Velocity profile for different values of Gr and Gc

The effects of velocity profiles for different values of time are illustrated in Figure 2.6. It is found that the velocity increases gradually with respect to time t . Moreover, the effect of time t on the velocity is dominant than other physical parameters like R , Sc and Gc or Gr .

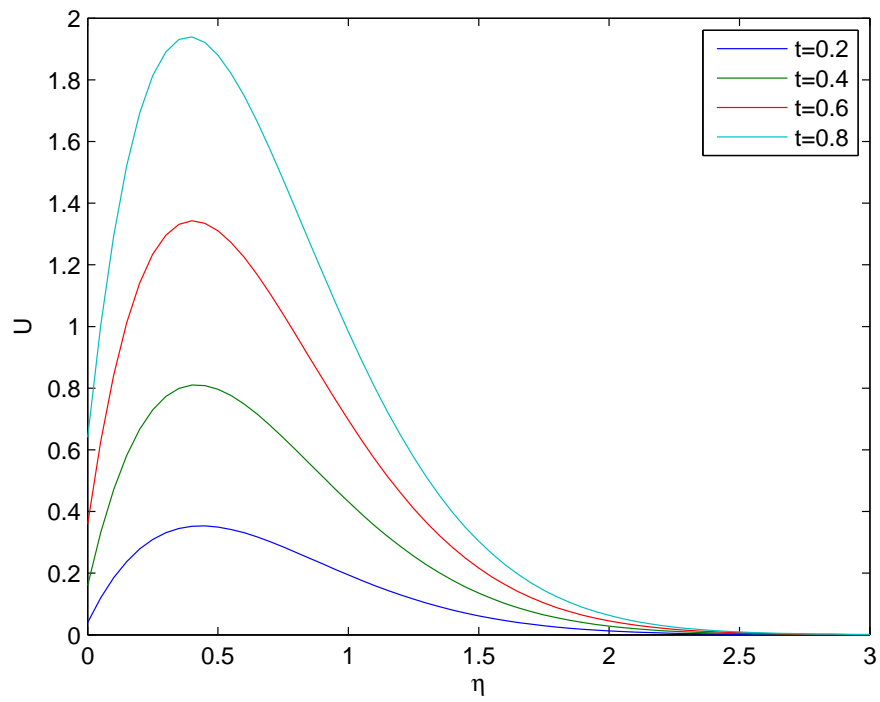


Figure 2.6 Velocity profile for different values of t

2.5 CONCLUSION

The theoretical solution of unsteady thermal radiation effects on flow past a parabolic starting motion of an infinite isothermal vertical plate with uniform mass flux, has been studied. The dimensionless governing equations are solved by the usual Laplace transform technique. The effect of different physical parameters like thermal radiation parameter, Schmidt number, thermal Grashof number, mass Grashof number and time are studied graphically. The conclusions of the study are as follows:

1. The velocity increases with increasing thermal Grashof number or mass Grashof number, but the trend is just reversed with respect to the thermal radiation parameter or Schmidt number.
2. The temperature of the plate increases with decreasing values of the thermal radiation parameter.
3. The plate concentration increases with decreasing values of the Schmidt number.